

# Extraordinary transmission caused by symmetry breaking

Dan Hu<sup>1,2</sup>, Chang-Qing Xie<sup>3</sup>, Ming Liu<sup>3</sup>, and Yan Zhang<sup>2\*</sup>

<sup>1</sup>*Department of Physics, Harbin Institute of Technology, Harbin, 150001 China*

<sup>2</sup>*Beijing Key Lab for Terahertz Spectroscopy and Imaging,*

*Key Laboratory of Terahertz Optoelectronics, Ministry of Education,*

*and Department of Physics, Capital Normal University, Beijing, 100048 China*

<sup>3</sup>*Laboratory of Micro-processing and Nanotechnology, Institute of Microelectronics, Chinese Academy of Sciences, Beijing, 100029 China*

(Dated: January 31, 2012)

The terahertz transmission properties of symmetrical and asymmetrical annular apertures arrays (AAAs) are investigated both experimentally and numerically. It is found that only odd order resonant modes are observed for the symmetrical structures but both odd and even order resonances can be shown for the asymmetrical structures. Breaking the symmetry of AAAs by gradually displacing the H-shaped AAAs to U-shaped AAAs allows an intensity modulation depth of 99% of the second order resonance. Simulation results verify the experimental conclusions well. This result provides a tremendous opportunity for terahertz wavelength tunable filtering, sensing, and near-field imaging.

PACS numbers: 78.20.Ci, 42.25.Bs

Since the extraordinary transmission (EOT) phenomenon of sub-wavelength metallic apertures arrays has been reported by Ebbesen and his co-workers [1, 2], it has been paid extensive attentions to understand the underlying physical mechanisms [3, 4]. Although it is still debated on the real mechanism of the EOT, surface plasmon polaritons (SPPs) originating from the coupling of light with the surface charges oscillation on the metal-dielectric interface [3] and the localized surface plasmon resonance (LSPR) excited on the hole ridge are recognized as the main possible contributions to the EOT [4]. Moreover, it has been shown that the transmission spectral response of sub-wavelength metallic apertures arrays are affected by the cell size [5], cell shape [6, 7], lattice periodicity [8], metal film thickness [9], the refractive index of the adjacent medium [10], as well as the polarization of incident light [11]. Annular aperture arrays (AAAs) have also been demonstrated to have EOT [12, 13]. The influence of geometric and structure parameters of the AAAs on the EOT properties has been extensively investigated. However, the influences of the symmetry of the AAAs on the EOT have not been reported. In this Letter, the transmission properties of the symmetric and asymmetric AAAs are investigated both experimentally and theoretically. The interactions of the terahertz (THz) electromagnetic radiation with the AAAs have been measured with the traditional THz time domain spectroscopy (TDS). The field distributions of the resonant wavelengths are simulated with the finite difference time domain (FDTD) method. The physical origin of the resonant enhanced transmission has been analyzed. It is found that the symmetry breaking can enhance the even order mode EOT.

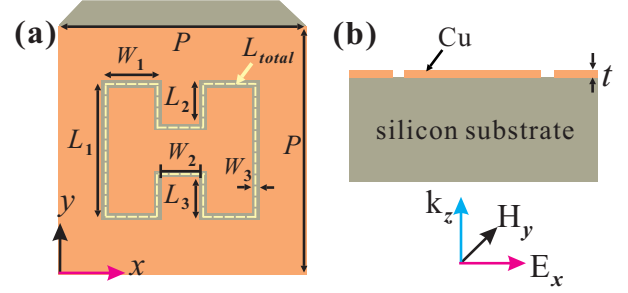


FIG. 1: Schematic view of the H-shaped AAAs. (a) Top view and (b) side view of the sample. The x-polarized THz illumination is also indicated in the figure.

The proposed AAAs structure is schematically shown in Fig. 1. It is a H-shaped annular slit. The outer arm length of the H-shaped slit is  $L_1$ , the upper and lower inner arm lengths are  $L_2$  and  $L_3$ , the outer and inner arm widths are  $W_1$  and  $W_2$ , respectively. The slit width is  $W_3 = 2.5\mu\text{m}$  and the period ( $\Lambda$ ) of the sample is  $200\mu\text{m}$ . This sample is symmetrical along both  $x$  and  $y$  directions. The total average circumference of the AAAs, which is the average length of out and inner edge of the slit, is denoted as  $L_{total}$ . The samples are fabricated onto a thin copper film ( $t = 200\text{nm}$ ) with the conventional photolithography and metallization processes. The substrate is a  $500\mu\text{m}$  thick doubly polished p-type silicon wafer.

The transmission spectra of the samples are measured by using a typical THz TDS. The THz wave pulses are generated from a dipole-type photoconductive antenna illuminated by a  $100\text{fs}$  laser with  $800\text{nm}$  center wavelength. The valid range of the system is  $0.2 - 2.6\text{THz}$ . The detection is achieved by a ZnTe crystal. For the reference, a bare silicon wafer identical to the one on which the AAAs are fabricated is used. The transmitted THz pulses are measured at normal incidence such that the

\*Electronic address: \*yzhang@mail.cnu.edu.cn

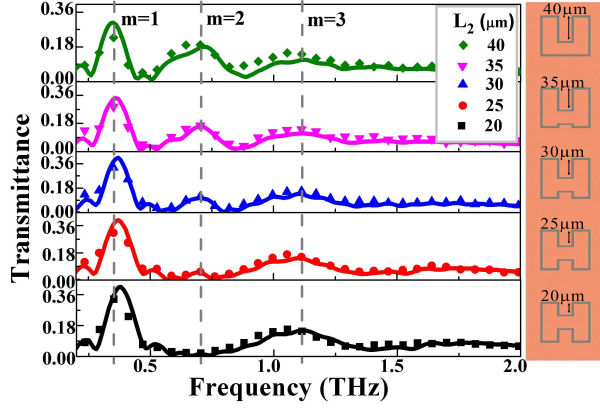


FIG. 2: Measured (symbol) and simulated (solid line) transmission spectra for AAAs with same average circumference  $L_{total}$  but different  $L_2$ .

electric and magnetic field of the incident radiation are in AAAs' plane. All measurements are done at room temperature and in a dry atmosphere to mitigate water absorption. The normalized transmittance is obtained by  $T(\nu) = |E_{sample}(\nu)/E_{ref}(\nu)|$ , where  $E_{sample}(\nu)$  and  $E_{ref}(\nu)$  are Fourier transformed transmitted electric field of the sample and reference pulses, respectively.

The transmission spectra of five samples with different  $L_2$  are shown in Fig. 2 with symbols. The parameters of the structures are selected as follows: The widths  $W_1$  and  $W_2$  are  $30\mu m$  and  $20\mu m$ , respectively. The length  $L_1$  is  $80\mu m$ . The length  $L_2$  increases from  $20\mu m$  to  $40\mu m$  with step of  $5\mu m$  and thus  $L_3$  reduces from  $20\mu m$  to  $0\mu m$ . The average circumference of the slit is kept as a constant as  $L_{total} = 390\mu m$ . For  $L_2 = L_3 = 20\mu m$ , the sample is H-shaped AAAs and symmetrical along both  $x$  and  $y$  directions. It can be seen that two resonance peaks at  $0.35THz$  and  $1.11THz$  appear in all transmission spectra. With  $L_2$  increasing, the symmetry of the structure along the  $y$  direction has been broken, the locations of these two peaks nearly unchanged but a new resonance peak appears at  $0.70THz$ . The transmission for  $0.70THz$  is enhanced from 1.97% for symmetrical structure to 17.5% for asymmetrical one, the intensity modulation depth is 99%.

For the AAAs structure, the localized surface plasmonics will be excited under the light illumination. The surface charges are assembled at the edge of the metal. Based on the basic idea of Ref. [14], the resonance appears when the following condition is satisfied:

$$f_m = \frac{mc}{n_{eff}L_{total}}, m = 1, 2, 3, \dots \quad (1)$$

where  $f_m$  is the resonant frequency,  $m$  is an integer which is the order of the resonant mode,  $c$  is the speed of light in vacuum,  $L_{total}$  is the average circumference of the AAAs, and  $n_{eff}$  is the effective refractive index for the localized

surface plasmonic wave. In our case,  $n_{eff}$  is approximately equal to  $(1.0 + n_{sub})/2$ ,  $n_{sub}$  is the refractive index of the substrate. Under this condition, the standing wave of the localized surface plasmon can be generated along the wedges of the metallic film. Furthermore, the distribution of localized surface plasmon should also satisfy the symmetry requirement of the samples. All samples considered here are symmetrical along the  $x$  direction and the illumination light is polarized along the  $x$  direction, thus the distribution of the assembled surface charges should be antisymmetrical along the  $x$  direction. If the sample is also symmetrical along the  $y$  direction, the distribution of the assembled surface charges should also be even symmetrical along the  $y$  direction. When the distribution of the assembled surface charges satisfy both the standing wave condition and symmetry condition, the corresponding transmission can be greatly enhanced. For all samples considered here, the odd mode (for example,  $m = 1$  or  $m = 3$ ) can easily satisfies these requirements no matter the sample is symmetrical along the  $y$  direction or not. However, if the resonant mode is even, the symmetry of the sample along the  $y$  direction will affect the distribution of the surface charges and hence the transmission amplitude. It requires the distribution of the surface charges is also symmetrical along the  $y$  direction. Thus, the standing wave condition for second mode can not be stratified any more, therefore, the transmission for the second resonant mode will be greatly reduced, as shown in Fig. 2 with  $L_2 = 20\mu m$ . But when the symmetry along the  $y$  direction is broken, the requirement of the symmetry of surface charge distribution along this direction does not exist, the standing wave of the localized surface plasmon can be generated and the resonant peak appears, as shown in Fig. 2 with  $L_2 = 40\mu m$ .

In order to get an insight into the nature of the resonant transmission for the proposed structures, the numerical simulations are carried out by using the FDTD approach [15]. The metal copper is described by the perfect electric conductor to fit its realistic characteristic in the terahertz range. The refractive indices of the air and substrate silicon are set as 1.0 and 3.31 in the simulations, respectively. The calculated transmission spectra are also shown in Fig. 2 with solid lines. It can be found that the simulation results correspond to the experiment measurements well. From the simulation results, it can also be found that the sample with  $L_2 = 20\mu m$  has two resonant peaks at  $0.35THz$  and  $1.11THz$ , which correspond to  $m = 1$  and  $m = 3$ , respectively. But the sample with  $L_2 = 40\mu m$  has three resonant peaks. A new peak corresponding to  $m = 2$  appears at  $0.70THz$ . With  $L_2$  increasing, the transmission for the second resonant mode enhanced.

Figure 3 presents the extremum electric field distributions at the aforementioned three resonant frequencies for samples with  $L_2$  equals  $20\mu m$ ,  $30\mu m$ , and  $40\mu m$ , respectively, which exhibits the distributions of the surface charges. When the structure is symmetrical along both

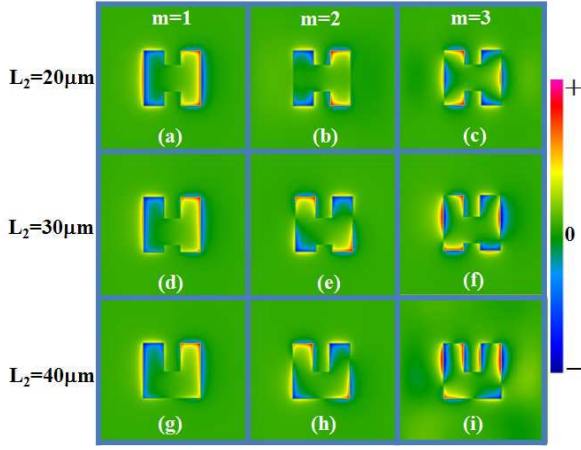


FIG. 3: Simulated  $E$  distributions on the interface between metal film and dielectric substrate silicon for three samples at three resonant wavelengths. The snapshot moment is when the field amplitude reaches its maximum. Only a unit cell on the  $x$ - $y$  plane is shown. The field quantity is normalized with respect to the incident field  $E_0$ .

$x$  and  $y$  directions, it can be found from Fig. 3(a)-(c) that the extremum electric field distributions are anti-symmetrical along the  $x$  direction but symmetrical along the  $y$  direction. These are natural results for satisfying the symmetrical requirement of the samples. For the odd modes  $m = 1$  and  $m = 3$  (correspond to Fig. 3(a) and (c), respectively), the standing waves are generated along the edges of the metallic film. One wave crest along the out side of slit in Fig. 3(a) and three crests in Fig. 3(c) can be found. However, in order to satisfy the symmetry condition along the  $y$  direction, the surface charge wave can not generate a standing wave with mode  $m = 2$ , as shown in Fig. 3(b). Only a temporarily electric field distribution is shown here and no standing wave distribution can be found. For the structure with  $L_2 = 40\mu\text{m}$ , the electric field distributions are also antisymmetrical along the  $x$  direction. Since the structure is not symmetrical along the  $y$  direction any more, the surface charges distributions are not required to be symmetrical along the  $y$  direction. There are 1, 2, and 3 standing waves generated for mode  $m = 1$  (Fig. 3(g)),  $m = 2$  (Fig. 3(h)) and  $m = 3$  (Fig. 3(i)), respectively. The even mode standing wave is formed and thus the corresponding transmission has been enhanced. It can be concluded that the resonant peak  $m = 2$  for the structure with  $L_2 = 40\mu\text{m}$  is

caused by the symmetry breaking along the  $y$  direction.

For further validation, the transmission spectra for another series of structures are calculated and shown in Fig. 4. The AAAs is cross shaped and the average circumference  $L_{ctotal}$  is still  $390\mu\text{m}$ . The girder is shifted from the middle to the bottom of the cross to break the symmetry along the  $y$  direction. It can be seen from the transmission spectra that the odd mode  $m = 1$  appears around  $0.35\text{THz}$  for all structures. However, the transmission intensity for second mode  $m = 2$  increases from  $0.39\%$

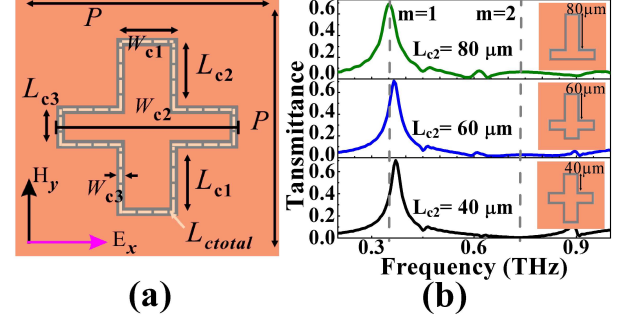


FIG. 4: (a) Schematic of cross shaped AAAs with fixed parameters:  $W_{c1} = 30\mu\text{m}$ ,  $W_{c1} = 100\mu\text{m}$ ,  $W_{c3} = 2.5\mu\text{m}$ ,  $L_{c1} + L_{c2} = 80\mu\text{m}$ ,  $L_{c3} = 20\mu\text{m}$ ,  $L_{ctotal} = 390\mu\text{m}$ , and the period  $\Lambda = 200\mu\text{m}$ . (b) Simulated spectra for cross shaped AAAs with same average circumference  $L_{ctotal}$  but different  $L_{c2}$ .

for symmetrical structure to  $6.5\%$  for the asymmetrical structure. These results also demonstrate that the symmetry breaking can enhance the odd mode resonance.

In summary, the transmission characteristics of the symmetrical and asymmetrical AAAs with narrow gap are investigated experimentally and numerically. The measured and simulated transmission spectra reveal that the resonant transmission are affected by the geometric structure. Both even and odd order modes can emerge for the asymmetrical AAAs but only odd order modes appears for the symmetrical AAAs. The appearance of the even mode is caused by the symmetry breaking. This research indicates a new freedom in tuning the electromagnetic response, which offers a path to design more robust plasmonic devices.

This work was supported by the 973 Program of China (No. 2011CB301801) and National Natural Science Foundation of China (No. 10904099 and 11174211).

- 
- [1] T. W. Ebbesen, H. J. Lezec, H. F. Ghaemi, T. Thio, and P. A. Wolff, *Nature (London)* **424**, 824 (1998).
  - [2] W. L. Barnes, A. Dereux, and T. W. Ebbesen, *Nature (London)* **391**, 667 (2003).
  - [3] H. F. Ghaemi, T. Thio, D. E. Grupp, T. W. Ebbesen, and H. J. Lezec, *Phys. Rev. B* **58**, 6779 (1998).
  - [4] S. A. Maier, *Plasmonics: Fundamentals and Applications*

- (Springer, New York, 2007).
- [5] K. L. V. Molen, F. B. Segerink, N. F. V. Hulst, and L. Kuipers, *Appl. Phys. Lett.* **85**, 4316 (2004).
- [6] J. W. Lee, M. A. Seo, D. J. Park, D. S. Kim, S. C. Jeoung, C. Lienau, Q. H. Park and P. C. M. Planken, *Opt. Express* **14**, 1253 (2006).
- [7] J. W. Lee, M. A. Seo, D. S. Kim, J. H. Kang, and Q-Han

- Park, Appl. Phys. Lett. **94**, 081102 (2009).
- [8] J. W. Lee, T. H. Park, P. Nordlander, and D. M. Mittleman, Appl. Phys. Lett. **97**, 261112 (2010).
  - [9] W. Wang, Y. L. Lu, R. J. Knize, K. Reinhardt, and S. C. Chen, Opt. Express **17**, 7361 (2009).
  - [10] A. K. Azad, Y. Zhao, and W. L. Zhang, Appl. Phys. Lett. **86**, 141102 (2005).
  - [11] J. B. Masson and G. Gallot, Phys. Rev. B **73**, 121401(R) (2006).
  - [12] Y. Poujet, J. Salvi, and F. I. Baida, Opt. Lett. **32**, 2942 (2007).
  - [13] X. C. Lu, J. G. Han, and W. L. Zhang, Opt. Lett. **35**, 070904 (2010).
  - [14] F. Neubrech, T. Kolb, R. Lovrincic, G. Fahsold, A. Puccia, J. Aizpurua, T. W. Cornelius, M. E. T. Molares, R. Neumann, and S. Karim, Appl. Phys. Lett. **89**, 253104 (2006).
  - [15] Simulations were performed using the software package CONCERTO 7.5R, developed by Vector Fields Limited, England, 2011.